



ELSEVIER

Contents lists available at ScienceDirect

## Surface &amp; Coatings Technology

journal homepage: [www.elsevier.com/locate/surfcoat](http://www.elsevier.com/locate/surfcoat)

# Effect of cavitation on corrosion behavior of HVOF-sprayed WC-10Co4Cr coating with post-sealing in artificial seawater

Ye Tian<sup>a,b,1</sup>, Haijun Zhang<sup>b,1</sup>, Xiuyong Chen<sup>b,c,\*</sup>, André McDonald<sup>d</sup>, Shuangjie Wu<sup>b</sup>, Tonghu Xiao<sup>a</sup>, Hua Li<sup>b,c,\*</sup>

<sup>a</sup> Faculty of Materials Science and Chemical Engineering, Ningbo University, Ningbo, 315211, Zhejiang, China

<sup>b</sup> Zhejiang Engineering Research Center for Biomedical Materials, Cixi Institute of Biomedical Engineering, Ningbo Institute of Materials Technology and Engineering, Chinese Academy of Sciences, Ningbo 315200, China

<sup>c</sup> Key Laboratory of Marine Materials and Related Technologies, Zhejiang Key Laboratory of Marine Materials and Protective Technologies, Ningbo Institute of Materials Technology and Engineering, Chinese Academy of Sciences, Ningbo 315201, China

<sup>d</sup> Department of Mechanical Engineering, University of Alberta, Edmonton, AB T6G 1H9, Canada

## ARTICLE INFO

## Keywords:

Cavitation  
Corrosion  
HVOF  
Sealing treatment  
WC-10Co4Cr coating

## ABSTRACT

This study aims to further improve the cavitation-corrosion performances of high-velocity oxygen-fuel (HVOF) sprayed WC-10Co4Cr coatings by post-sealing treatment with epoxy resin using a vacuum impregnation method. Compared with the as-sprayed coatings with a porosity of 2.52%, the sealed WC-10Co4Cr coatings with a much lower porosity of 0.78% were successfully fabricated. The sealed coatings showed significantly enhanced corrosion and cavitation resistance tested in artificial seawater compared to those of the as-sprayed coatings. Further cavitation-corrosion testing under cavitation and quiescence conditions showed that the corrosion rate of both the as-sprayed coating and sealed coating was reduced under cavitation condition. Furthermore, a mechanism was suggested to illustrate the effect of cavitation on corrosion behavior of the coatings. The sealing treated WC-10Co4Cr coatings show encouraging promises as cavitation-corrosion resistance layers for marine structures.

## 1. Introduction

In marine environments, the materials for ship are exposed to corrosion [1] and cavitation [2–4]. To prevent this, thermal sprayed coatings have been widely used for corrosion and cavitation protection of the materials (such as AISI 1045 steel, 316L stainless steel and low carbon steel) [5–7]. However, there are generally many defects (such as pores and cracks) in the actual coatings [8–11]. Thus, corrosion and cavitation begin from the pre-existing defect and expand to the whole coating. Post-sealing processes can significantly reduce the porosity of thermal sprayed coatings, thereby enhancing its corrosion and cavitation resistance. For example, Wang et al. [12] reported the effect of sealing treatment on the corrosion resistance of high-velocity oxygen-fuel (HVOF) sprayed Fe-based amorphous metallic coatings. The results presented that the AlPO<sub>4</sub> sealant could penetrate the coating effectively and the corrosion resistance of sealed coating was greatly enhanced. Deng et al. [13] found that the mechanical properties and cavitation

performance of plasma spray Al<sub>2</sub>O<sub>3</sub>-13%TiO<sub>2</sub> coatings were significantly improved after sealing process with epoxy resin which could successfully penetrated into the whole Al<sub>2</sub>O<sub>3</sub>-13%TiO<sub>2</sub> coating (approximately 300 μm).

To the current, many studies have been carried out on cavitation-corrosion behavior and mechanism. For example, Hong et al. [14] studied the synergistic effect of cavitation and corrosion of HVOF sprayed FeCrSiBMn coatings. The results showed that cavitation reduced the corrosion resistance of the coatings, and mechanical effect was the main factor of the synergistic effect. Park et al. [15] reported the influence of cavitation on the corrosion behavior of arc sprayed Al-3Mg coating. The results showed that the corrosion rate of the arc sprayed Al-3Mg coating was significantly accelerated under cavitation condition. Bakhshandeh et al. [16] studied the cavitation-corrosion behavior of Ni/β-SiC nanocomposite coatings under cavitation condition in 3.5% NaCl solution. The results presented that cavitation accelerated anodic reaction on 17-4 precipitation hardening stainless steel

\* Corresponding authors at: Zhejiang Engineering Research Center for Biomedical Materials, Cixi Institute of Biomedical Engineering, Ningbo Institute of Materials Technology and Engineering, Chinese Academy of Sciences, Ningbo 315200, China.

E-mail addresses: [chenxiuyong@nimte.ac.cn](mailto:chenxiuyong@nimte.ac.cn) (X. Chen), [lihua@nimte.ac.cn](mailto:lihua@nimte.ac.cn) (H. Li).

<sup>1</sup> These authors contributed equally to this work.

<https://doi.org/10.1016/j.surfcoat.2020.126012>

Received 30 January 2020; Received in revised form 29 May 2020; Accepted 2 June 2020

Available online 05 June 2020

0257-8972/ © 2020 Elsevier B.V. All rights reserved.

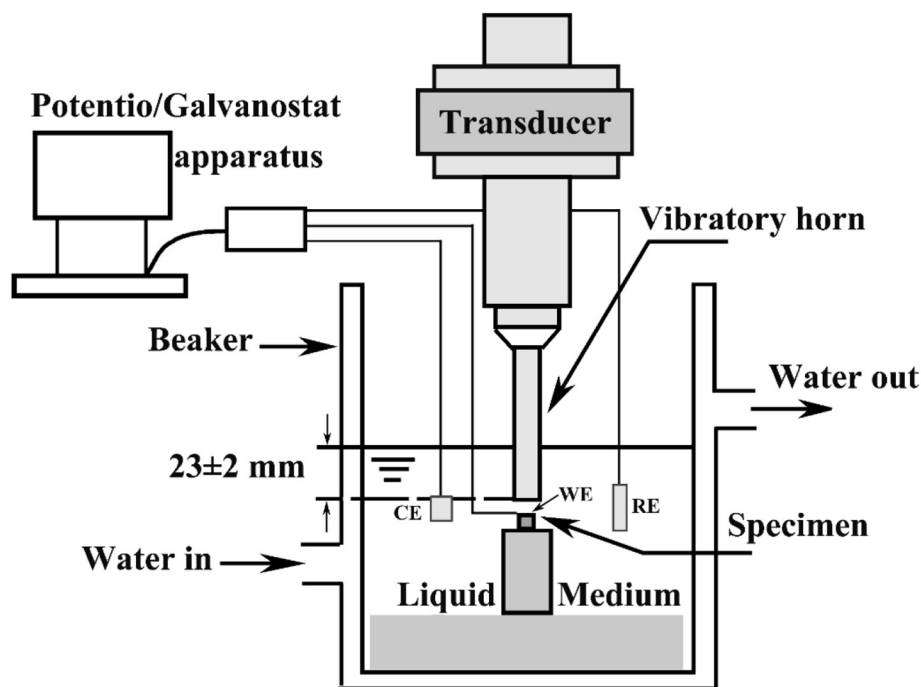


Fig. 1. Schematic illustration showing the cavitation-corrosion test system.

(17-4 PH SS) and cathodic reaction on the Ni/ $\beta$ -SiC coating. The results of the above studies show that cavitation complicates the surface of the material, which causes the influence of cavitation on corrosion to be difficult to predict, and it is possible to promote and suppress, which may be related to the type and defect of the material.

HVOF sprayed WC-10Co4Cr coating has attracted great attention due to its good cavitation resistance property [17,18]. So far, few studies have been reported on the effect of cavitation on the corrosion behavior of both as-sprayed WC-10Co4Cr coating and sealing treated WC-10Co4Cr coating in marine environments. We hypothesized that the corrosion resistance of the WC-10Co4Cr coating under corrosion and corrosion-cavitation condition after sealing treatment would be improved. To confirm the hypothesis, in this study, WC-10Co4Cr coatings were prepared on 316L stainless steel substrates (316L SS) by HVOF and then sealed with epoxy resin using a vacuum impregnation method [13]. The cavitation-only performance of the 316L SS, as-sprayed coating and sealed coating was performed by ASTM standard G32-16 method, and corrosion performance of the materials under cavitation and quiescence was tested by cavitation-corrosion equipment [19] in artificial seawater (ASW). The corrosion behavior of the materials under cavitation and quiescence conditions was investigated.

## 2. Experimental procedure

### 2.1. Materials

The substrates used in this research were 316L SS plates with a 20 mm diameter and 10 mm height. WC-10Co4Cr powders (WOKA-C 3652, Spherical, 15 to 45  $\mu\text{m}$ ) were provided by Oerlikon Metco Surface Technology (Shanghai) Co. Ltd., China. ASW (NaCl: 24.53 g/L,  $\text{MgCl}_2$ : 5.20 g/L,  $\text{Na}_2\text{SO}_4$ : 4.09 g/L,  $\text{CaCl}_2$ : 1.16 g/L, KCl: 0.695 g/L,  $\text{NaHCO}_3$ : 0.201 g/L, KBr: 0.101 g/L,  $\text{H}_3\text{BO}_3$ : 0.027 g/L,  $\text{SrCl}_2$ : 0.025 g/L, NaF: 0.003 g/L) was prepared based on the ASTM Standard D1141-98 (2003) [20]. Epoxy resin (number average molecular weight  $\sim$ 600) and curing agent (Triethylenetetramine) were obtained from Aladdin Reagent Co., Ltd., China.

### 2.2. Coating preparation and characterization

WC-10Co4Cr coatings were deposited on 316L SS by using an HVOF spray system (CJK5, Castolin Eutectic, Germany). Before thermal spraying, the surfaces of the substrates were grit blasted with 60 mesh (250  $\mu\text{m}$ )  $\text{Al}_2\text{O}_3$  and cleaned. The HVOF spray system was performed using kerosene as the fuel gas and nitrogen as the powder carrier gas. The details of the spray parameters used in this study have been described in detail elsewhere [21]. Briefly, the spray parameters used in this research were conducted at a spray distance of 300 mm, an oxygen flow rate of 845  $\text{mL}\cdot\text{min}^{-1}$ , a kerosene flow rate of 480  $\text{mL}\cdot\text{min}^{-1}$ , a carrier gas flow rate of 9.9  $\text{mL}\cdot\text{min}^{-1}$ , and a powder feed rate of 11.9  $\text{g}\cdot\text{min}^{-1}$ . To ensure good sealing performance for the as-sprayed coatings, the epoxy resin and curing agent with an optimum volume ratio of 7:1 were used. The epoxy resin and curing agent were well mixed, and then evenly spread on the as-sprayed coatings. After that, the coatings were put into a vacuum oven for 70 min, allowing the epoxy resin to fully penetrate the coating gaps, and then cured at 170  $^\circ\text{C}$  for 1 h [13]. A field emission scanning electron microscope (FESEM, FEI Quanta FEG 250, the Netherlands) equipped with Energy Dispersive Spectrometer (EDS) was utilized to characterize the cross section morphology of the as-sprayed coating and sealed coating. The cross section images of the coatings were analyzed using Adobe Photoshop CS6 to calculate their porosities.

### 2.3. Cavitation, corrosion and cavitation-corrosion tests

Cavitation-corrosion tests were conducted by using an ultrasound device (Guobiao Ultrasonic Equipment Co., Ltd., Hangzhou, China) with an electrochemical test system [19], according to the ASTM standard G32-16 [22]. The vibration frequency used in this study was 20 kHz, the peak amplitude was 50  $\mu\text{m} \pm 5\%$ , and the sample was immersed in ASW which was maintained at 25  $\pm 2$   $^\circ\text{C}$ . For cavitation-only testing, the materials were polished to a mirror finish, cleaned with acetone, dried in warm air, and finally weighed using an analytical balance (Mettler 220, Toledo Instruments Co., Ltd., Shanghai, China) with an accuracy of 0.1 mg. The schematic of the cavitation-corrosion test apparatus is shown in Fig. 1. The distance between the studied

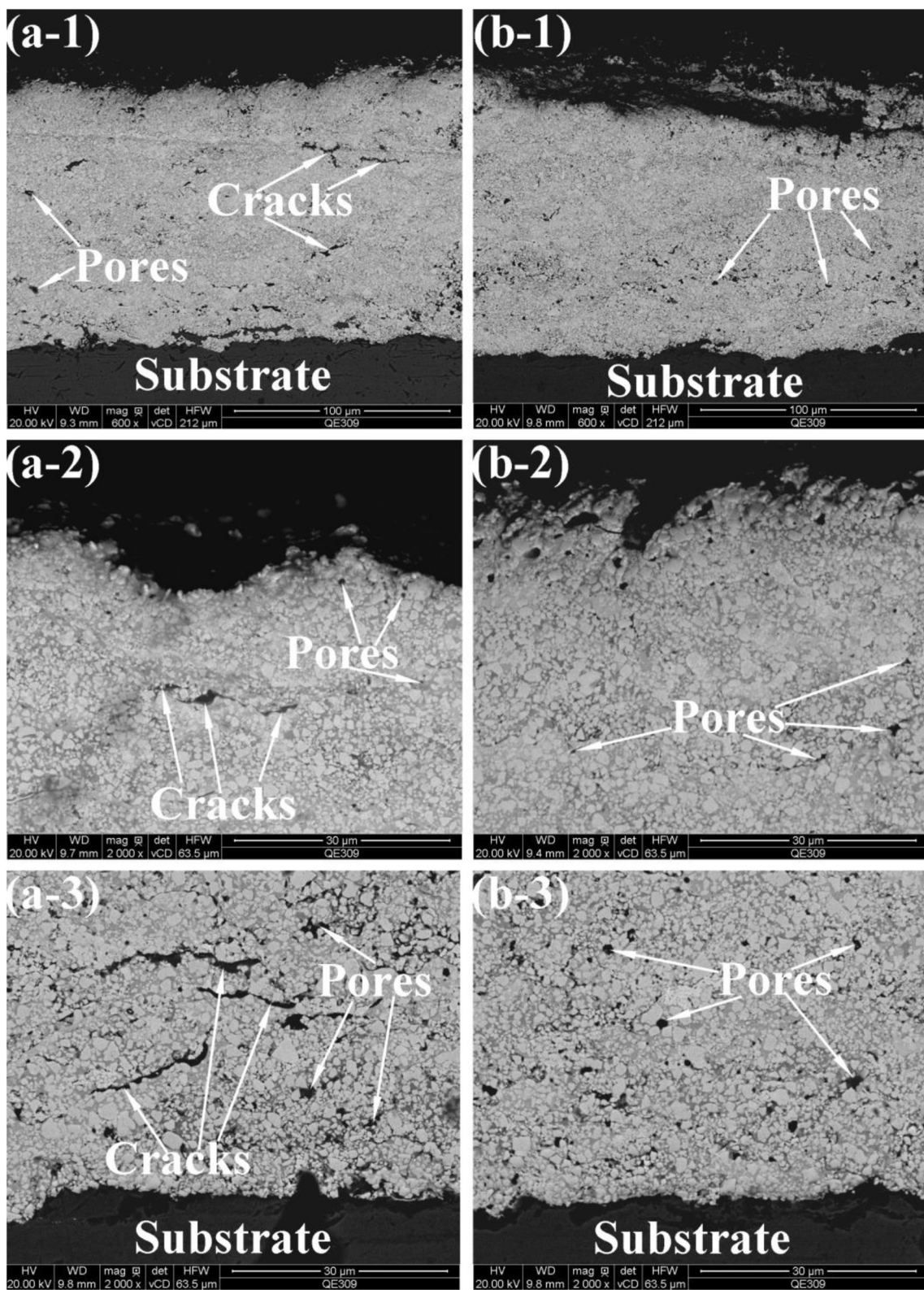


Fig. 2. FESEM cross sectional morphologies of the (a) as-sprayed coating, and (b) sealed coating. (-2: the top of the coating; -3: the bottom region of the coating).

Table 1  
Chemical compositions of the as-sprayed coating and sealed coating.

Samples	C (wt%)	O (wt%)	Cr (wt%)	Co (wt%)	W (wt%)
As-sprayed coating	8 ± 2	0	6 ± 3	14 ± 4	72 ± 8
Sealed coating	12 ± 2	4 ± 2	5 ± 3	12 ± 6	67 ± 8

sample surface and the horn tip was 1 mm. The horn was immersed in ASW at a depth of  $23 \pm 2$  mm. The electrochemical data were measured with a conventional three-electrode system (Solartron Modulab, 2100A, UK). A platinum electrode was used as the counter electrode (CE), a saturated calomel electrode was used as the reference electrode (RE), and a  $10 \times 10 \text{ mm}^2$  sample working surface was used as the

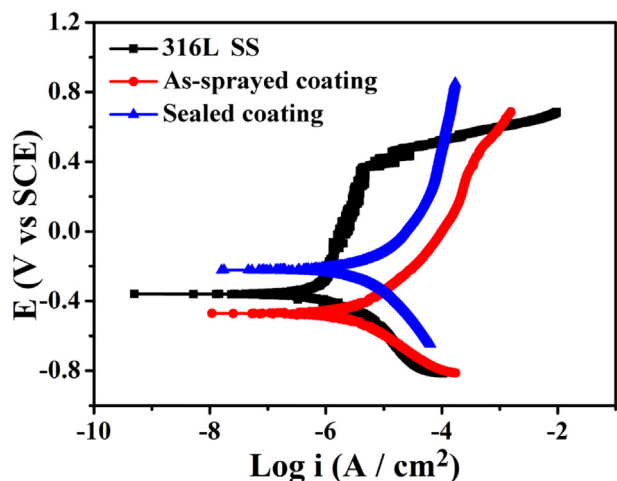


Fig. 3. Potentiodynamic polarization curves measured under the corrosion-only in artificial seawater solution.

Table 2

Corrosion current densities ( $i_{corr}$ ) and corrosion potentials ( $E_{corr}$ ) of the 316L SS, as-sprayed coating and sealed coating in ASW solution under quiescence and cavitation conditions.

Samples	$E_{corr}$ (mV)		$i_{corr}$ ( $\mu\text{A}\cdot\text{cm}^{-2}$ )	
	Quiescence	Cavitation	Quiescence	Cavitation
316L SS	-0.36	-0.28	$0.23 \pm 0.01$	$0.16 \pm 0.02$
As-sprayed coating	-0.48	-0.39	$2.9 \pm 0.1$	$1.1 \pm 0.2$
Sealed coating	-0.23	-0.31	$1.4 \pm 0.1$	$0.78 \pm 0.06$

Table 3

The charge transfer resistance ( $R_{ct}$ ) value of the 316L SS, as-sprayed coating and sealed coating in ASW solution under quiescence and cavitation conditions.

Samples	$R_{ct}$ ( $\text{k}\Omega\cdot\text{cm}^2$ )	
	Quiescence	Cavitation
316L SS	$86.3 \pm 0.8$	$1122 \pm 16$
As-sprayed coating	$2.9 \pm 0.1$	$7.9 \pm 0.5$
Sealed coating	$16.1 \pm 0.1$	$22 \pm 2$

Table 4

The fitted results for EIS of the 316L SS, as-sprayed coating and sealed coating.

EIS parameters	316L SS	As-sprayed coating	Sealed coating
$R_s$ ( $\Omega\cdot\text{cm}^2$ )	$10.9 \pm 0.2$	$9.6 \pm 0.2$	$11.4 \pm 0.2$
$Q_{coat}$ ( $\mu\text{F}\cdot\text{cm}^{-2}\cdot\text{s}^{-n_1}$ )	-	$32 \pm 2$	$13.2 \pm 0.8$
$R_{coat}$ ( $\Omega\cdot\text{cm}^2$ )	-	$818 \pm 1$	$126.5 \pm 0.9$
$n_1$	0.83	0.71	0.89
$Q_{dl}$ ( $\mu\text{F}\cdot\text{cm}^{-2}\cdot\text{s}^{-n_2}$ )	$94 \pm 2$	$157 \pm 4$	$5.3 \pm 0.2$
$R_{ct}$ ( $\text{k}\Omega\cdot\text{cm}^2$ )	$86 \pm 1$	$2.9 \pm 0.1$	$16.1 \pm 0.1$
$n_2$	-	0.86	0.67
$\chi^2$ ( $\times 10^{-3}$ )	5.01	2.02	7.54

working electrode (WE), and electrochemical data were processed using Nova 2.1 software. For corrosion-only tests, all the samples were sealed by ethylene-vinyl acetate copolymer (EVA) to gain a testing surface area of  $10 \times 10 \text{ mm}^2$  and immersed in ASW solution for 1 h before electrochemical signals were acquired. For cavitation-corrosion tests, the samples were firstly immersed in ASW for 1 h. Potentiodynamic polarization curves were obtained with a potential scan rate of 0.5 mV/s under quiescent and cavitation conditions. To obtain the effect of cavitation on the open circuit potential ( $E_{ocp}$ ) of samples in the ASW solution,  $E_{ocp}$  was tested under quiescent and cavitation conditions. For

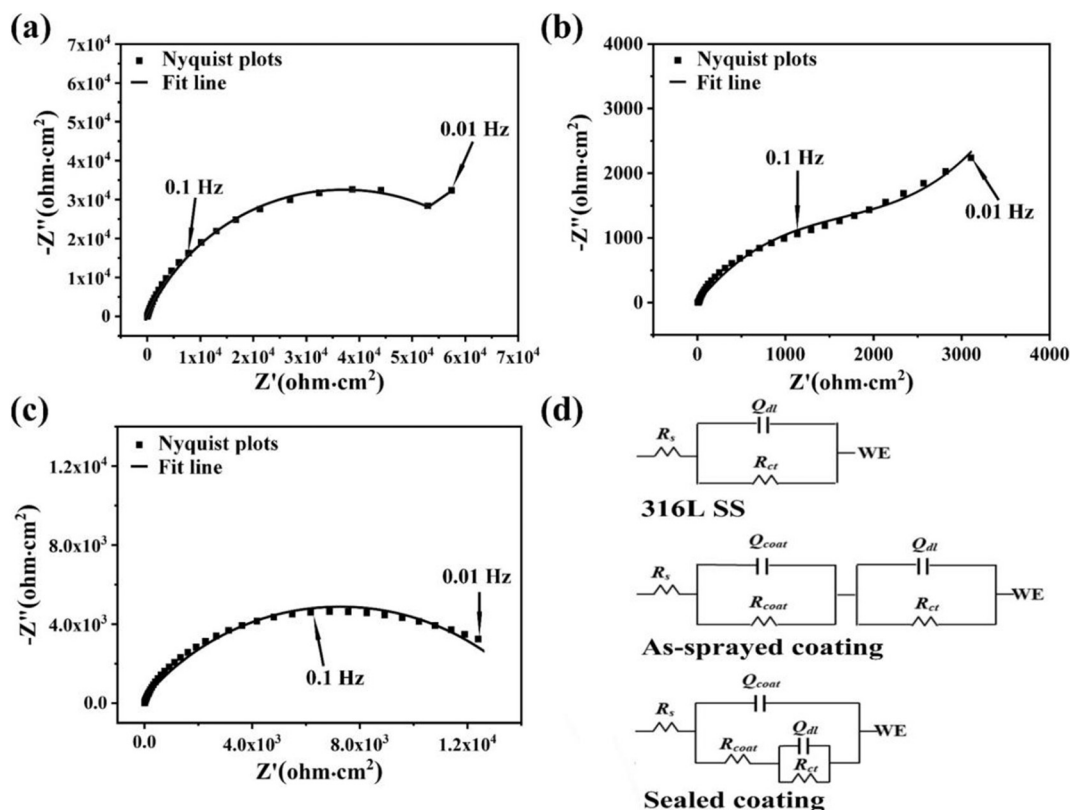


Fig. 4. Nyquist diagrams (a-c) and equivalent circuit models (d) of the 316L SS, as-sprayed coating, sealed coating in artificial seawater solution.  $R_s$ : solution resistance,  $Q_{dl}$ : capacitance of the double layer,  $R_{ct}$ : charge transfer resistance,  $Q_{coat}$ : capacitance of the coating,  $R_{coat}$ : resistance of the coating.

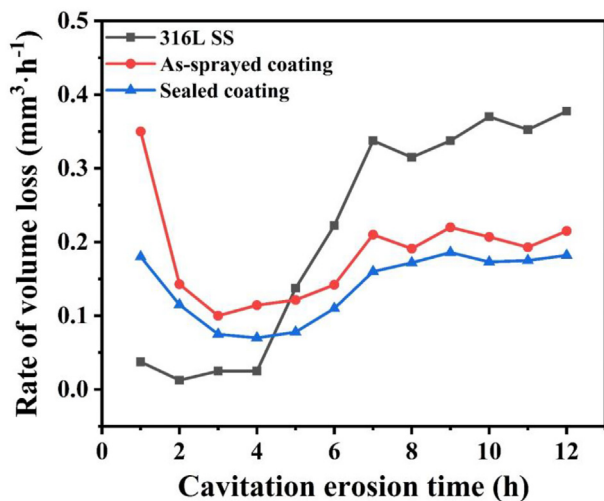


Fig. 5. The rate of volume loss of the 316L SS, as-sprayed coating and sealed coating after 12 h of cavitation in artificial seawater.

electrochemical impedance spectroscopy (EIS) test, the experimental samples were exposed to cavitation condition for 5 h before testing. EIS test was recorded in the frequency range of  $10^5$  Hz to  $10^{-2}$  Hz using a sinusoidal potential excitation signal with an amplitude of 20 mV [23–25]. After the EIS test, the acquired data were fitted and analyzed using a ZSimpWin software based on equivalent circuit models. Each testing was repeated three times to ensure reproducibility.

### 3. Results and discussion

#### 3.1. Microstructural characterization

Typical cross section backscattered electron (BSE) SEM images of the as-sprayed and sealed coatings are shown in Fig. 2. As observed in Fig. 2a-1 and b-1, the thickness of the coatings was approximately 125  $\mu\text{m}$ . Pores and cracks can be clearly observed in the as-sprayed coating both localized respective the top (Fig. 2a-2) and bottom region (Fig. 2a-3) of the coating. The as-sprayed coating exhibited some degree of laminar microstructures (Fig. 2a-2). Besides, some micro-cracks were found among the splats of the as-sprayed coating, which may be attributed to excessive shrinkage rates of fully molten particles at a rapid cooling rate. The defective parts (pores and cracks) could significantly reduce the cavitation and corrosion resistance of the as-sprayed coating [7,17]. Sealing treatment is a commonly used method to reduce the pores and cracks of thermal spray coatings [26,27]. After sealing treatment (Fig. 2b), it is worth to notice that no cracks were observed, and most of the larger pores have been sealed by epoxy resin, even though a few small pores can still be found (Fig. 2b-2 and b-3). The average porosities of the as-sprayed coating and the sealed coating were approximately 2.52% and 0.78%, respectively. A similar trend was reported by a previous study [21]. For further confirmation, this study carried out an EDS analysis of the as-sprayed and sealed coatings. EDS results are listed in Table 1, showing that sealed coating has significantly higher carbon contents and oxygen contents compared to those of the as-sprayed coating, indicating that the epoxy penetrated the as-sprayed coating after sealing.

#### 3.2. Effect of sealing treatment on corrosion behavior of the coatings

The potentiodynamic polarization curves of the 316L SS, as-sprayed coating and sealed coating in the ASW solution are shown in Fig. 3. The corresponding electrochemical values are presented in Table 2. The corrosion potentials ( $E_{corr}$ ) of the 316L SS, as-sprayed coating and sealed coating are about  $-0.36$ ,  $-0.48$  and  $-0.23$  V, respectively. The

corrosion current density ( $i_{corr}$ ) of the sealed coating is  $1.1 \mu\text{A}\cdot\text{cm}^{-2}$ , which is smaller than that of the as-sprayed coating ( $2.9 \mu\text{A}\cdot\text{cm}^{-2}$ ). It is worth noting that the  $i_{corr}$  of the as-sprayed coating in this study was much lower than that of HVOF sprayed WC-10Co4Cr coating on AISI 1018 low-carbon steel substrate which was reported in a previous study [6]. This could be related to the different substrates used. The sealed coating showed low corrosion current density and high corrosion potential comparing to those of the as-sprayed coating, suggesting better corrosion resistance, which maybe attributes to its low porosity. Previous studies [18,28,29] have shown that pores and cracks defects, especially penetrating pores in the HVOF coating, exhibited an important effect on the corrosion resistance of the HVOF coatings. Moreover, the difference in open circuit potential between reinforcing particulate (WC particles) and soft metal matrix (Co and Cr) causes micro-galvanic corrosion between the two phases in ASW environments. The WC particles become cathodic and, resulting in the corrosion of anodic binder materials [30,31].

Fig. 4 presents the Nyquist plots (Fig. 4a–c) and equivalent circuit models (Fig. 4d) for the 316L SS, as-sprayed coating and sealed coating in ASW solution. The charge transfer resistance ( $R_{ct}$ ) values were listed in Table 3. The  $R_{ct}$  of the 316L SS, as-sprayed coating and sealed coating were approximately  $86.3 \pm 0.8$ ,  $2.9 \pm 0.1$  and  $16.1 \pm 0.1 \text{ k}\Omega\cdot\text{cm}^2$ , respectively. As can be seen that the  $R_{ct}$  value of the coating was significantly increased after sealing treatment, which is consistent with the potentiodynamic polarization curves (Fig. 3). To elucidate the impedance response of the corrosion behavior in ASW solution, equivalent circuit models are provided in Fig. 4d. The 316L SS fits the one-time constant model, R(QR). And the as-sprayed coating conforms to the two-time constant model (R(QR)(QR)). Consistent with previous reports [32,33], the EIS spectra of the as-sprayed coating show two partly overlapped semicircles. The parallel  $R_{coat}$ - $Q_{coat}$  group simulates the high-frequency semicircle which represents the open pores of the as-sprayed coating are filled by the electrolyte in anodized systems. The parallel  $R_{ct}$ - $Q_{dl}$  group simulates the low-frequency semicircle, associated with the electrolyte-electrode interface reaction, and it shows the anodic dissolution of the substrate [32,34]. However, after sealing treatment of the as-sprayed coating, the porosity of the coating is significantly reduced which close the system against the penetration of the electrolyte to the coating. Therefore, the coating after sealing is suitable for the R(Q(R(QR))) model, which is consistent with a previous study [7].  $R_s$  is solution resistance,  $Q_{dl}$  is capacitance of the double layer,  $R_{ct}$  is charge transfer resistance,  $Q_{coat}$  is capacitance of the coating,  $R_{coat}$  is resistance of the coating. The values of the impedance parameters are summarized in Table 4. It indicates that the sealed coating displays a better corrosion resistance than that of the as-sprayed coating.

#### 3.3. Effect of sealing treatment on cavitation-only behavior of the coatings

The volume loss rate of the 316L SS, as-sprayed coating and sealed coating are shown in Fig. 5. At the beginning of the cavitation tests, the volume loss rates of the as-sprayed coating and sealed coating were significantly higher than that of the 316L SS. This phenomenon was probably attribute to the protruding particles and pores of the original surface which were easier to be eroded and removed [35]. The volume loss rate of the coatings reached a plateau after erosion for 7 h. It is worth noting that the volume loss rate of the sealed coating was significantly lower than that of the as-sprayed coating and the 316L SS after erosion for 5 h. This is probably related to the porosity reduction of the coating after sealing treatment [36]. In order to further investigate the cavitation behavior of the coatings, the surface morphologies of the materials before and after cavitation were obtained, as shown in Fig. 6. Before the cavitation test, no obvious defects could be seen on the polished 316L SS, as-sprayed coating and sealed coating surface (Fig. 6a-1, b-1, and c-1). After 12 h of cavitation erosion testing, significant pinholes and big craters were observed on the surface of the 316L SS (Fig. 6a-2). The eroded surface of the 316L SS was the most

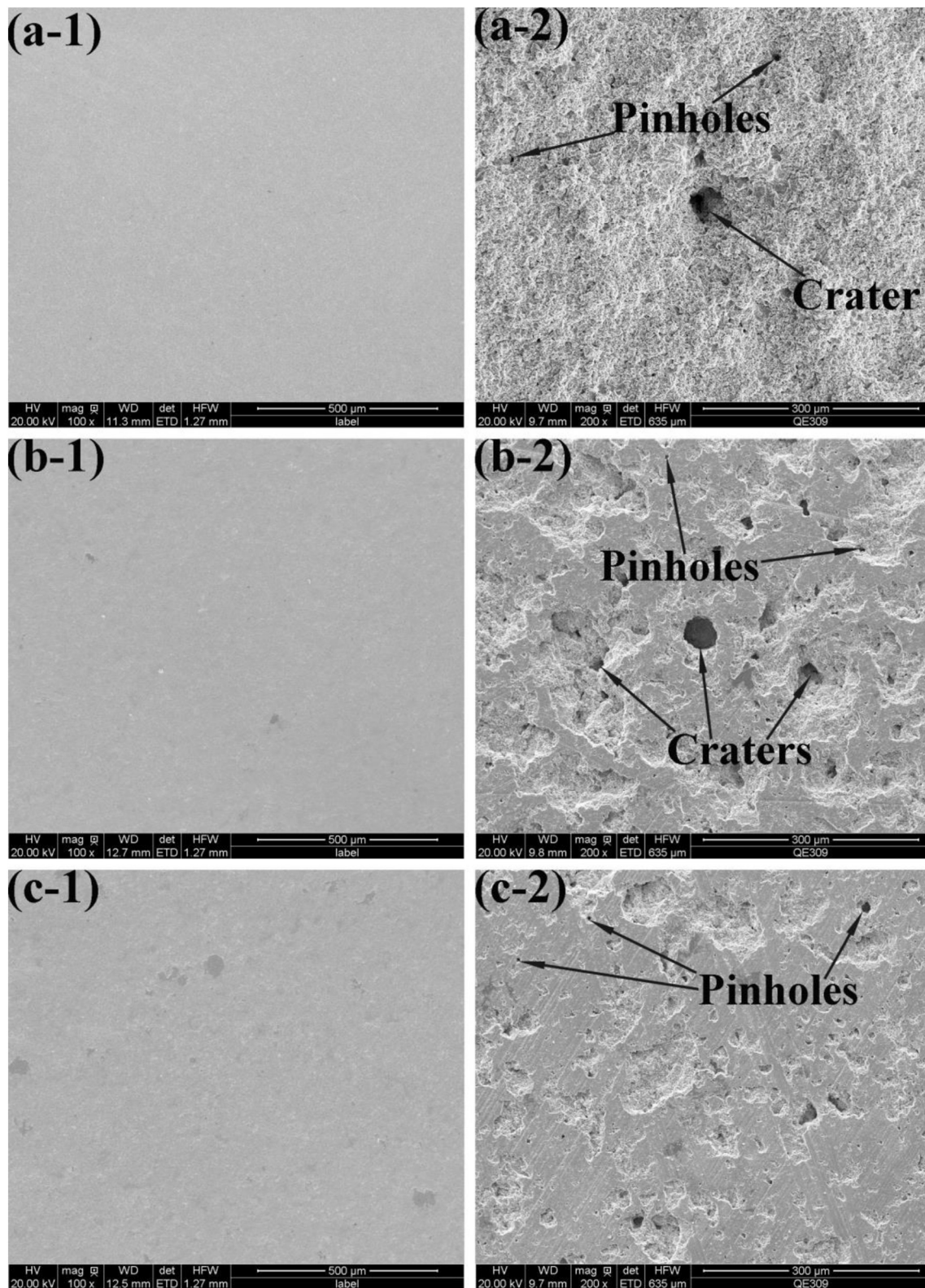


**Fig. 6.** The surface morphologies of the (a) 316L SS, (b) as-sprayed coating and (c) sealed coating (–1) before and (–2) after 12 h of cavitation in artificial seawater.

seriously damaged material when compared to the as-sprayed coating (Fig. 6b-2) and sealed coating (Fig. 6c-2). For the as-sprayed coating, pinholes and craters were presented on the eroded surface (Fig. 6b-2). Relatively small cavitation pits were observed on the surface of the sealed coating (Fig. 6c-2). Moreover, compared with the surface morphology on the eroded surfaces of the sealed coating, more serious

damage was presented in the as-sprayed coating. This result is consistent with the volume loss rate data (Fig. 5). The results demonstrated that sealing treatment had a significant effect on their cavitation erosion property because of that the porosity of the coating was effectively reduced. This result was similar to that of a recent study reported by Deng et al. [13].

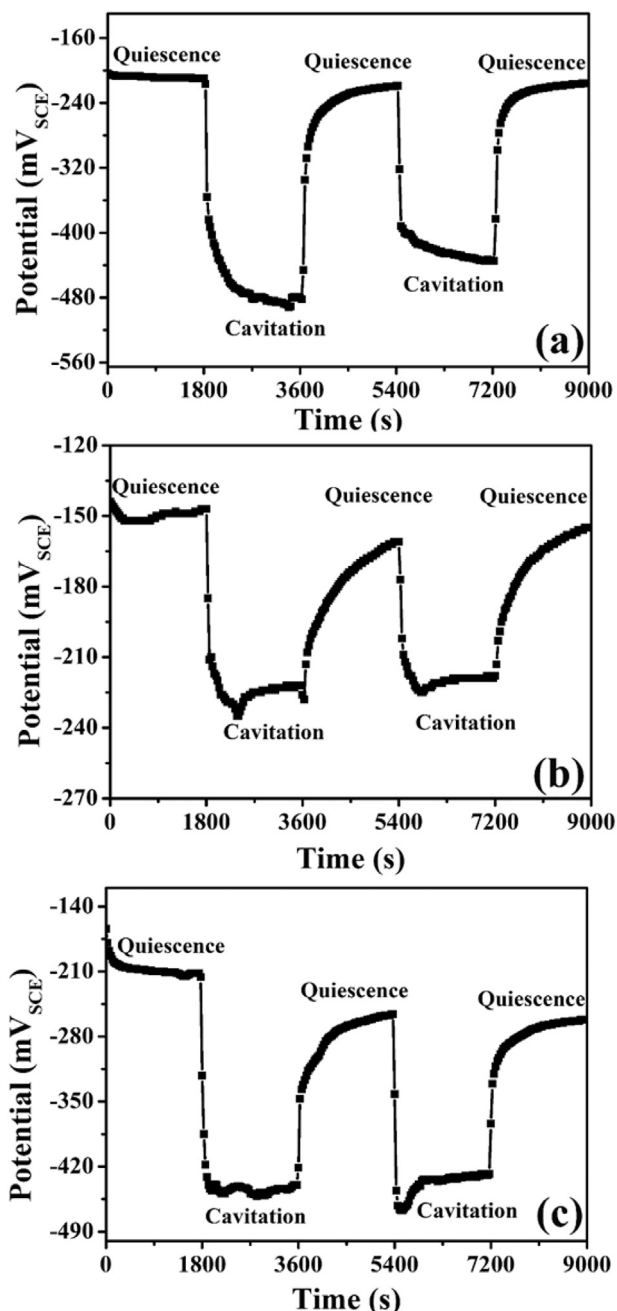


Fig. 7.  $E_{ocp}$  vs. time of the (a) 316L SS, (b) as-sprayed coating, and (c) sealed coating in artificial seawater under quiescence and cavitation conditions.

### 3.4. Effect of cavitation on corrosion behavior of the as-sprayed coatings and sealed coatings in ASW

The effect of cavitation on the  $E_{ocp}$  of the 316L SS, as-sprayed coating and sealed coating in the ASW solution is shown in Fig. 7. The  $E_{ocp}$  values of the 316L SS, as-sprayed coating and sealed coating under quiescence were  $-200$ ,  $-150$  and  $-210$  mV, respectively. During the cavitation of 1800 s, the  $E_{ocp}$  values of the 316L SS, as-sprayed coating and sealed coating were  $-480$ ,  $-230$  and  $-450$  mV, respectively. This means that cavitation shifted the  $E_{ocp}$  of the materials in the active direction. The influence of cavitation on the corrosion behavior of the materials can be generally related to two competing effects including corrosion film or product (such as loose oxide layers or passive protective films) detachment and an increase of mass transport (such as oxygen) [37,38]. A negative  $E_{ocp}$  shift is presented if the former effect

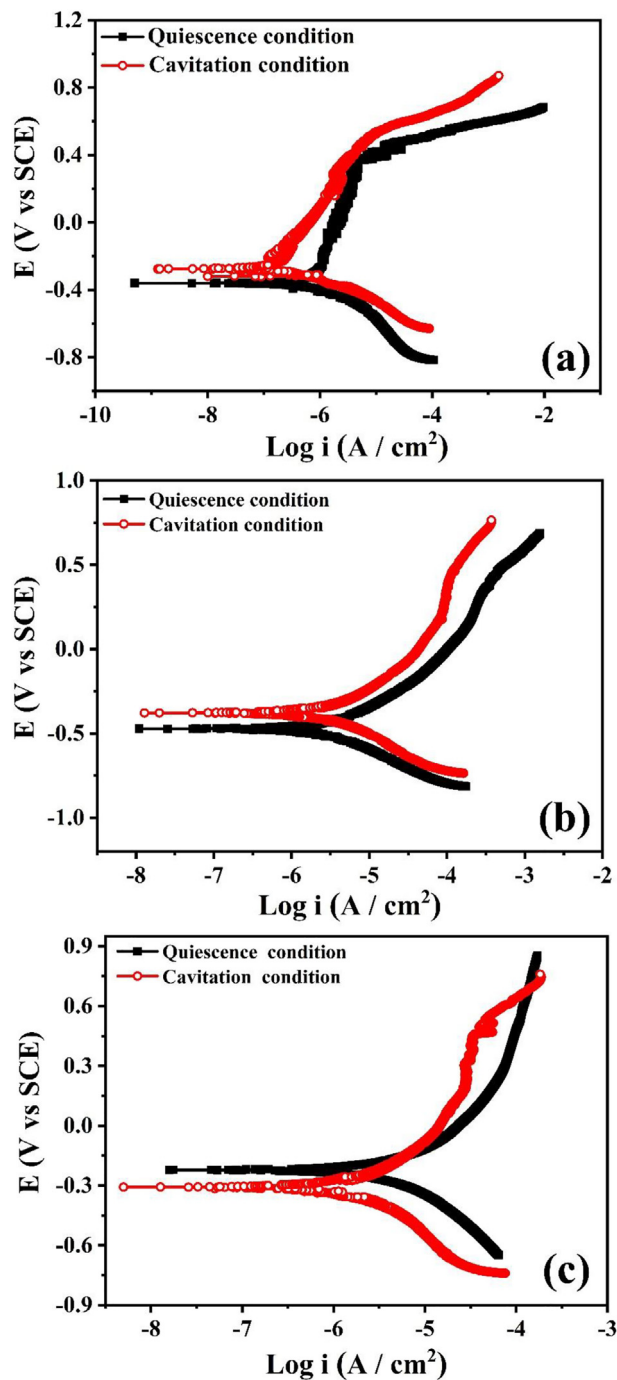


Fig. 8. Potentiodynamic polarization curves of the (a) 316L SS, (b) as-sprayed coating, and (c) sealed coating in artificial seawater under quiescence and cavitation conditions.

plays a key role by exposing the fresh surface of the studied material, while a positive  $E_{ocp}$  shift occurs if the latter dominates by increasing oxygen supply to the material surface. In general, a lower  $E_{ocp}$  corresponds to a higher corrosion rate [39,40]. However, the surface of the material is an unstable state under cavitation condition. Luo et al. [24] studied the effect of cavitation on the corrosion behavior of 20SiMn low alloy steel on a 3% sodium chloride solution. The results showed that cavitation shifted the  $E_{ocp}$  to the noble direction, but cavitation also increases the cathodic corrosion current and decreases the  $R_{ct}$ , indicating that cavitation has a positive effect on corrosion. Similar results were also reported by Jiang et al. [41]. So, it is not enough to judge the corrosion performance of the material under cavitation

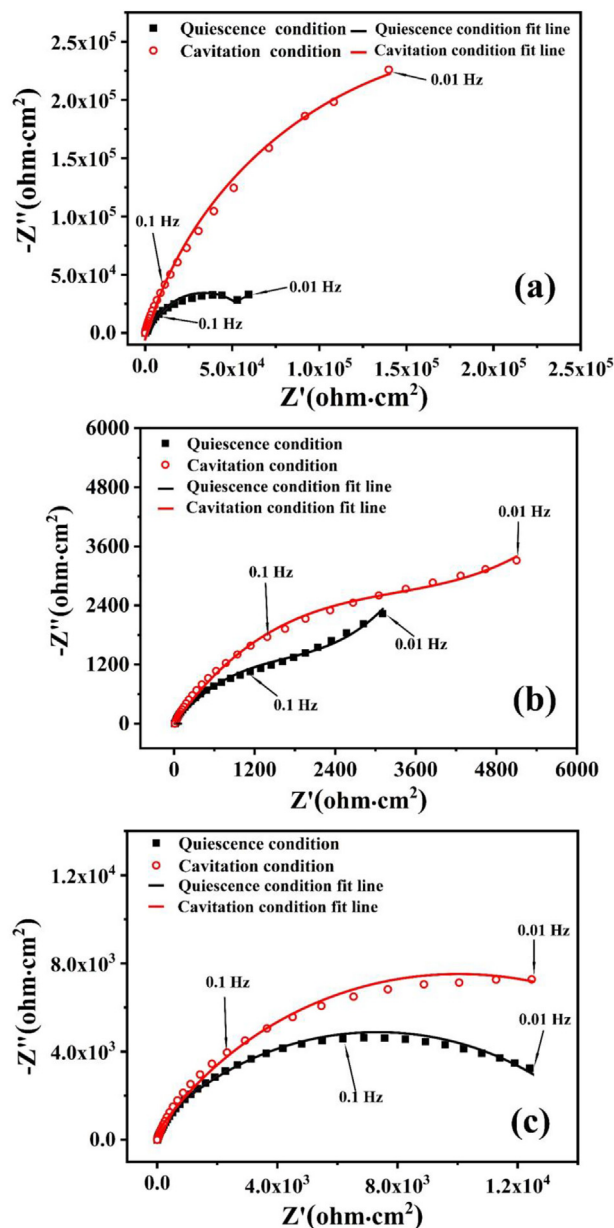


Fig. 9. Nyquist plots of the (a) 316L SS, (b) as-sprayed coating, and (c) sealed coating in artificial seawater under quiescence and cavitation conditions.

conditions only based on  $E_{ocp}$  results.

To further investigate the effect of cavitation on corrosion of the coatings, potentiodynamic polarization and electrochemical impedance spectroscopy were carried out. Fig. 8 and Table 2 show the potentiodynamic polarization curves under quiescence and cavitation conditions for the 316L SS, as-sprayed coating and sealed coating in the ASW solution. It can be seen that cavitation strongly affected the polarization behavior of the 316L SS (Fig. 8a). The  $i_{corr}$  values of the 316L SS under quiescent and cavitation conditions were 0.23 and 0.16  $\mu\text{A}\cdot\text{cm}^{-2}$ , respectively. A similar trend was found for the as-sprayed coating (Fig. 8b). The  $i_{corr}$  values of the as-sprayed coating under quiescence and cavitation conditions were 2.9 and 1.1  $\mu\text{A}\cdot\text{cm}^{-2}$ , respectively. For the sealed coating (Fig. 8c), interestingly, unlike the 316L SS and as-sprayed coating, both the anodic and cathodic reactions of the sealed coating were reduced. The  $i_{corr}$  values of the sealed coating under quiescent and cavitation conditions were 1.4 and 0.78  $\mu\text{A}\cdot\text{cm}^{-2}$ , respectively. It is worth noting that the  $i_{corr}$  of the 316L SS and the as-sprayed coating at given cathodic potentials under cavitation-corrosion

condition were larger than that measured under corrosion condition, while the  $i_{corr}$  of the 316L SS and the as-sprayed coating at given anodic potentials under cavitation-corrosion condition were smaller than that measured under corrosion condition (Fig. 8a and b). This phenomenon occurred because cavitation mainly accelerated the cathodic reaction process and decreased the anodic reaction process of the 316L SS and the as-sprayed coating, however, cavitation decreased the anodic reaction and the cathodic reaction process of the sealed coating.

Fig. 9 shows the Nyquist plots for the 316L SS, as-sprayed coating and sealed coating under quiescence and cavitation conditions. At the entire frequency, the impedance is expressed in the form of a semi-circular capacitance in the impedance spectrum, and the diameter of the semicircle represents the  $R_{ct}$  [42,43]. The shape of the impedance spectrum does not change, which means that the material does not change the electrochemical mechanism [23,24]. Any change in the electrochemical mechanism will be considered as two EIS semicircles in the test results [6]. It can be seen from Fig. 9a that cavitation strongly affected the impedance spectra of the 316L SS. Both under quiescence and cavitation conditions for the 316L SS, at the higher frequencies, the Nyquist plots exhibited a capacitive loop, but at the lower frequencies, the Nyquist plots exhibited a diffusion-controlled charge transfer [44]. The  $R_{ct}$  of the 316L SS under quiescence conditions was about 86.3  $\text{k}\Omega\cdot\text{cm}^2$ , while the  $R_{ct}$  of 316L SS significantly increased under cavitation condition (1122  $\text{k}\Omega\cdot\text{cm}^2$ ) (Table 3). For the as-sprayed coating (Fig. 9b), the  $R_{ct}$  increased from 2.9 (under quiescence condition) to 7.9  $\text{k}\Omega\cdot\text{cm}^2$  (under cavitation condition), indicating that the corrosion rate of the as-sprayed coating was reduced under cavitation condition, which is different from Hong's research [17]. Generally, cavitation accelerates the diffusion of oxygen to the surface of the material, which leads to the production of a passivation film and reduces the corrosion rate, but cavitation also damages the passivation film and increases the corrosion rate, these two competitive effects exist simultaneously in cavitation conditions [37,38]. Different research results may be due to the difference in the distance of the sample from the cavitation vibration horn. Due to the different models of ultrasonic cavitation equipment, the samples are typically fixed below the vibrating horn at a distance of 0.5 to 2 mm [45–50]. Hong's research used a distance of 0.5 mm, but in this study a distance of 1 mm was used. The closer to the vibrating horn, the more destructive the cavitation jet is [51]. It can be seen from Fig. 9c that cavitation also strongly affected the  $R_{ct}$  of the sealed coating. The  $R_{ct}$  values of the sealed coating under quiescent and cavitation conditions were 16.1 and 22  $\text{k}\Omega\cdot\text{cm}^2$  (Table 3), respectively, suggesting that cavitation also reduced the corrosion rate of the sealed coating in ASW solution. That is to say, the sealed coating shows a better anti-corrosion performance than that of the as-sprayed coating under corrosion-only and cavitation-corrosion conditions. This phenomenon could be explained that cavitation enhanced the passivation ability and reduced the pitting corrosion possibility of the materials [38]. Although the  $R_{ct}$  values of the stainless steel was higher than those of the as-sprayed coating and sealed coating under quiescence and cavitation conditions, mechanical cavitation was the main cause of damage of the materials (such as stainless steel) for flow passage components of ships. And the main goal of adding the sealed WC-10Co4Cr coating on the stainless steel substrate was for improving the cavitation resistance property.

### 3.5. Failure mechanisms

The possible failure mechanisms of the as-sprayed coating and sealed coating are illustrated in Fig. 10. For the original cross section of the as-sprayed coating, which usually comprised of a few defects (pores and cracks) [18]. For the as-sprayed coating under corrosion-only condition, oxygen and chloride could easily infiltrate into the coating along with the pores and cracks, and gradually caused the serious corrosion of the as-sprayed coating [52]. For the sealed coating under corrosion-only condition, due to the epoxy resin sealing the cracks and

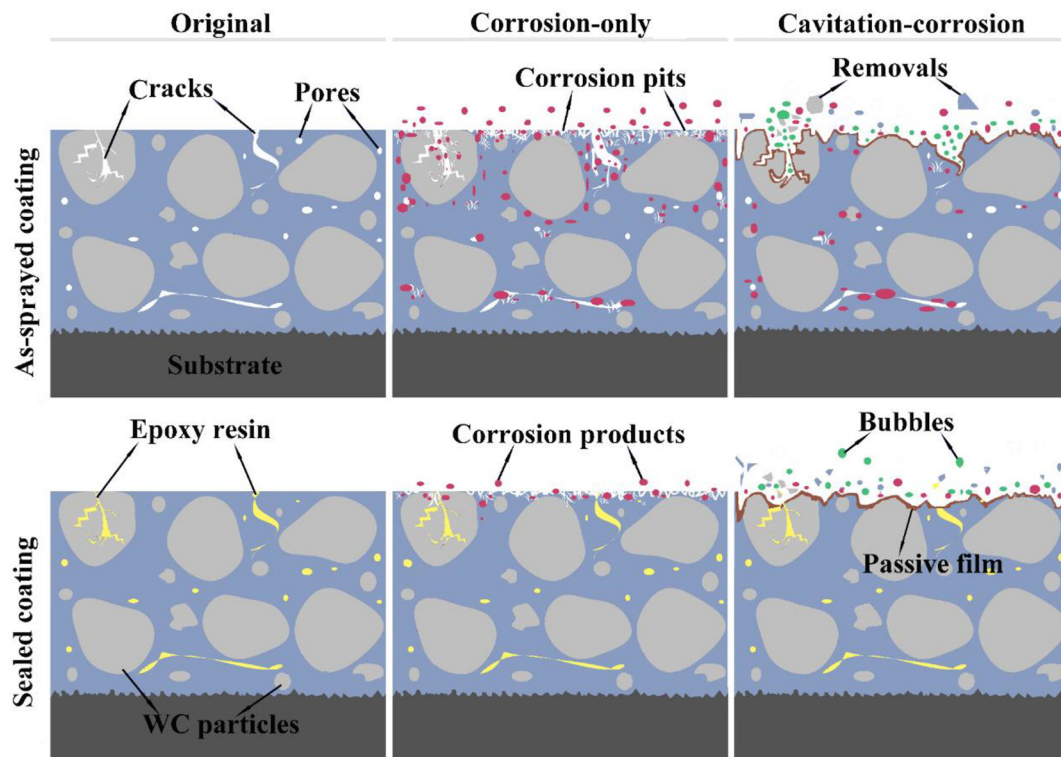


Fig. 10. Schematic diagram of the effect of cavitation on corrosion behavior of the as-sprayed coating and sealed coating.

pores in the coating, the corrosive medium cannot penetrate into the sealed coating, the permeability of oxygen and chloride was greatly reduced, thereby improving the corrosion resistance of the sealed coating. For the as-sprayed coating under cavitation-corrosion condition, cavitation pits would preferentially grow at defects in the coating. Although the micro-jet generated by cavitation would peel off the passivation film ( $\text{Cr}_2\text{O}_3$ ,  $\text{CoO}$ ,  $\text{WO}_3$  [18,53–56]) of the as-sprayed coating, this would also accelerate the diffusion and conduction of oxygen, resulting in the formation of the passivation film. This is a competitive behavior under cavitation-corrosion condition [37,38,57]. Under cavitation-corrosion condition, when the rate of passivation film production is greater than the rate of passivation film peeling, the corrosion rate of the coating decreases. For the sealed coating under cavitation-corrosion condition, due to the reduced defects of the coating by sealing treatment, the rate of penetration of oxygen and chloride ions into the coating decreases, which reduces the corrosion rate of the sealed coating.

#### 4. Conclusions

High-velocity oxygen-fuel sprayed WC-10Co4Cr coatings and post-sealing treated WC-10Co4Cr coatings with epoxy resin were fabricated and their corrosion and cavitation resistance performances were studied in artificial seawater. In addition, the effect of cavitation on the corrosion behavior of the tested coating samples was investigated. It was found that the sealed coatings exhibited higher corrosion and cavitation resistance than those of the as-sprayed coatings and cavitation reduced the corrosion rate of the tested samples in artificial seawater solution. Furthermore, a mechanism was suggested to illustrate the effect of cavitation on corrosion behavior of the coatings. The results showed that post-sealing treatment and cavitation had a significant impact on their corrosion performance.

#### CRediT authorship contribution statement

**Ye Tian:**Methodology, Investigation, Writing - original draft,

Software.**Haijun Zhang:**Methodology, Investigation, Formal analysis, Software.**Xiuyong Chen:**Conceptualization, Writing - review & editing, Formal analysis, Supervision.**André McDonald:**Writing - review & editing.**Shuangjie Wu:**Methodology, Investigation, Data curation.**Tonghu Xiao:**Supervision.**Hua Li:**Writing - review & editing, Supervision.

#### Declaration of competing interest

The authors declare that we have no known competing financial interests or personal relationships that could have appeared to influence the work reported in this paper.

#### Acknowledgments

This study was supported by the Chinese Academy of Sciences President's International Fellowship Initiative (grant # 2020VEA0005), CAS-Iranian Vice Presidency for Science and Technology Joint Research Project (grant # 174433KYSB20160085), and a Natural Sciences and Engineering Research Council of Canada Discovery Grant (grant # NSERC RGPIN-2018-04298).

#### References

- [1] J. Bhandari, F. Khan, R. Abbassi, V. Garaniya, R. Ojeda, Modelling of pitting corrosion in marine and offshore steel structures-a technical review, *J. Loss Prevent. Proc.* 37 (2015) 39–62.
- [2] J.W. Lindau, D.A. Boger, R.B. Medvitz, R.F. Kunz, Propeller cavitation breakdown analysis, *J. Fluid. Eng.* 127 (2005) 995–1002.
- [3] Z. Zhu, S. Fang, Numerical investigation of cavitation performance of ship propellers, *J. Hydrodyn.* 24 (2012) 347–353.
- [4] R.J.K. Wood, Erosion-corrosion interactions and their effect on marine and offshore materials, *Wear* 261 (2006) 1012–1023.
- [5] H. Zhang, X. Chen, Y. Gong, Y. Tian, A. McDonald, H. Li, In-situ SEM observations of ultrasonic cavitation erosion behavior of HVOF-sprayed coatings, *Ultrason. Sonochem.* 60 (2020) 104760.
- [6] G.C. Saha, T.I. Khan, The corrosion and wear performance of microcrystalline WC-10Co-4Cr and near-nanocrystalline WC-17Co high velocity oxy-fuel sprayed coatings on steel substrate, *Metall. Mater. Trans. A* 41 (2010) 3000–3009.

- [7] S. Hong, Y. Wu, Y. Zheng, B. Wang, W. Gao, J. Lin, Microstructure and electrochemical properties of nanostructured WC-10Co-4Cr coating prepared by HVOF spraying, *Surf. Coat. Tech.* 235 (2013) 582–588.
- [8] M. Barletta, G. Bolelli, B. Bonferroni, L. Lusvarghi, Wear and corrosion behavior of HVOF-sprayed WC-CoCr coatings on Al alloys, *J. Therm. Spray Techn.* 19 (2010) 358–367.
- [9] Y. Liu, W. Liu, Y. Ma, S. Meng, C. Liu, L. Long, S. Tang, A comparative study on wear and corrosion behavior of HVOF- and HVAF-sprayed WC-10Co-4Cr coatings, *Surf. Eng.* 33 (2016) 63–71.
- [10] A. Milanti, H. Koivuluoto, P. Vuoristo, G. Bolelli, F. Bozza, L. Lusvarghi, Microstructural characteristics and tribological behavior of HVOF-sprayed novel Fe-based alloy, *Coatings* 4 (2014) 98–120.
- [11] V. Matikainen, K. Niemi, H. Koivuluoto, P. Vuoristo, Abrasion, erosion and cavitation erosion wear properties of thermally sprayed alumina based coatings, *Coatings* 4 (2014) 18–36.
- [12] Y. Wang, S. Jiang, Y. Zheng, W. Ke, W. Sun, J. Wang, Effect of porosity sealing treatments on the corrosion resistance of high-velocity oxy-fuel (HVOF)-sprayed Fe-based amorphous metallic coatings, *Surf. Coat. Tech.* 206 (2011) 1307–1318.
- [13] W. Deng, G. Hou, S. Li, J. Han, X. Zhao, X. Liu, Y. An, H. Zhou, J. Chen, A new methodology to prepare ceramic-organic composite coatings with good cavitation erosion resistance, *Ultrason. Sonochem.* 44 (2018) 115–119.
- [14] S. Hong, Y. Wu, J. Zhang, Y. Zheng, Y. Zheng, J. Lin, Synergistic effect of ultrasonic cavitation erosion and corrosion of WC-CoCr and FeCrSiBm coatings prepared by HVOF spraying, *Ultrason. Sonochem.* 31 (2016) 563–569.
- [15] I.C. Park, S.J. Kim, Synergistic effect of cavitation-erosion and corrosion of Al and Al-Mg alloy coatings by arc thermal spraying in sea water, *Sci. Adv. Mater.* 8 (2016) 1827–1831.
- [16] H.R. Bakhshandeh, S.R. Allahkaram, A.H. Zabihi, An investigation on cavitation-corrosion behavior of Ni/beta-SiC nanocomposite coatings under ultrasonic field, *Ultrason. Sonochem.* 56 (2019) 229–239.
- [17] S. Hong, Y. Wu, J. Zhang, Y. Zheng, Y. Qin, J. Lin, Ultrasonic cavitation erosion of high-velocity oxygen-fuel (HVOF) sprayed near-nanostructured WC-10Co-4Cr coating in NaCl solution, *Ultrason. Sonochem.* 26 (2015) 87–92.
- [18] Q. Wang, S. Zhang, Y. Cheng, J. Xiang, X. Zhao, G. Yang, Wear and corrosion performance of WC-10Co4Cr coatings deposited by different HVOF and HVAF spraying processes, *Surf. Coat. Tech.* 218 (2013) 127–136.
- [19] J. Basumatary, M. Nie, R.J.K. Wood, The synergistic effects of cavitation erosion-corrosion in ship propeller materials, *J. Bio. Tribo. Corros.* 1 (2015) 12.
- [20] ASTM, D1141-98, Standard Practice for the Preparation of Substitute Ocean Water, ASTM International, West Conshohocken, Pennsylvania, 2013.
- [21] H. Zhang, Y. Gong, X. Chen, A. McDonald, H. Li, A comparative study of cavitation erosion resistance of several HVOF-sprayed coatings in deionized water and artificial seawater, *J. Therm. Spray Techn.* 28 (2019) 1060–1071.
- [22] ASTM, G32-16, Standard Test Method for Cavitation Erosion Using Vibratory Apparatus, ASTM International, West Conshohocken, Pennsylvania, 2016.
- [23] S. Hong, Y. Wu, J. Zhang, Y. Zheng, Y. Qin, J. Lin, Effect of ultrasonic cavitation erosion on corrosion behavior of high-velocity oxygen-fuel (HVOF) sprayed near-nanostructured WC-10Co-4Cr coating, *Ultrason. Sonochem.* 27 (2015) 374–378.
- [24] S.Z. Luo, Y.G. Zheng, M.C. Li, Z.M. Yao, W. Ke, Effect of cavitation on corrosion behavior of 20SiMn low-alloy steel in 3% sodium chloride solution, *Corros. Sci.* 59 (2003) 597–605.
- [25] S.L. Jiang, Y.G. Zheng, Z.M. Yao, Cavitation erosion behaviour of 20SiMn low alloy steel in Na<sub>2</sub>SO<sub>4</sub> and NaHCO<sub>3</sub> solutions, *Corros. Sci.* 48 (2006) 2614–2632.
- [26] S.J. Kim, S.J. Lee, I.J. Kim, S.K. Kim, M.S. Han, S.K. Jang, Cavitation and electrochemical characteristics of thermal spray coating with sealing material, *T. Nonferr. Metal. Soc.* 23 (2013) 1002–1010.
- [27] S. Liscano, L. Gil, M.H. Staia, Correlation between microstructural characteristics and the abrasion wear resistance of sealed thermal-sprayed coatings, *Surf. Coat. Tech.* 200 (2005) 1310–1314.
- [28] P.H. Suegama, C.S. Fugivara, A.V. Benedetti, J. Fernández, J. Delgado, J.M. Guilemany, Electrochemical behavior of thermally sprayed stainless steel coatings in 3.4% NaCl solution, *Corros. Sci.* 47 (2005) 605–620.
- [29] I.B. Singh, D.P. Mandal, M. Singh, S. Das, Influence of SiC particles addition on the corrosion behavior of 2014 Al-Cu alloy in 3.5% NaCl solution, *Corros. Sci.* 51 (2009) 234–241.
- [30] G.C. Saha, T.I. Khan, Comparative abrasive wear study of HVOF coatings obtained by spraying WC-17Co microcrystalline and duplex near-nanocrystalline cermet powders, *J. Eng. Mater. Tech.* 133 (2011) 041002.
- [31] J.E. Cho, S.Y. Hwang, K.Y. Kim, Corrosion behavior of thermal sprayed WC cermet coatings having various metallic binders in strong acidic environment, *Surf. Coat. Tech.* 200 (2006) 2653–2662.
- [32] M. Barletta, G. Bolelli, B. Bonferroni, L. Lusvarghi, Wear and corrosion behavior of HVOF-sprayed WC-CoCr coatings on Al alloys, *J. Therm. Spray Techn.* 19 (2010) 358–367.
- [33] P.H. Suegama, C.S. Fugivara, A.V. Benedetti, J.M. Guilemany, J. Fernández, J. Delgado, The influence of gun transverse speed on electrochemical behaviour of thermally sprayed Cr<sub>3</sub>C<sub>2</sub>-NiCr coatings in 0.5 M H<sub>2</sub>SO<sub>4</sub> solution, *Electrochim. Acta* 49 (2004) 627–634.
- [34] J.M. Guilemany, J. Fernández, J. Delgado, A.V. Benedetti, F. Climent, Effects of thickness coating on the electrochemical behaviour of thermal spray Cr<sub>3</sub>C<sub>2</sub>-NiCr coatings, *Surf. Coat. Tech.* 153 (2002) 107–113.
- [35] L. Qiao, Y. Wu, S. Hong, J. Zhang, W. Shi, Y. Zheng, Relationships between spray parameters, microstructures and ultrasonic cavitation erosion behavior of HVOF sprayed Fe-based amorphous/nanocrystalline coatings, *Ultrason. Sonochem.* 39 (2017) 39–46.
- [36] S.J. Kim, S.J. Lee, I.J. Kim, S.K. Kim, M.S. Han, S.K. Jang, Cavitation and electrochemical characteristics of thermal spray coating with sealing material, *T. Nonferr. Metal. Soc.* 23 (2013) 1002–1010.
- [37] C.T. Kwok, F.T. Cheng, H.C. Man, Cavitation erosion and corrosion behavior of laser-aluminized mild steel, *Surf. Coat. Tech.* 200 (2006) 3544–3552.
- [38] B. Vyas, I.L.H. Hansson, The cavitation erosion-corrosion of stainless steel, *Corros. Sci.* 30 (1990) 761–770.
- [39] Y. Ye, Z. Liu, W. Liu, D. Zhang, H. Zhao, L. Wang, X. Li, Superhydrophobic oligoaniline-containing electroactive silica coating as pre-process coating for corrosion protection of carbon steel, *Chem. Eng. J.* 348 (2018) 940–951.
- [40] F. Eliyan, F.A. Alfantazi, On the theory of CO<sub>2</sub> corrosion reactions - investigating their interrelation with the corrosion products and API-X100 steel microstructure, *Corros. Sci.* 85 (2014) 380–393.
- [41] S.L. Jiang, Y.G. Zheng, Z.M. Yao, Cavitation erosion behavior of 20SiMn low alloy steel in Na<sub>2</sub>SO<sub>4</sub> and NaHCO<sub>3</sub> solutions, *Corros. Sci.* 48 (2006) 2614–2632.
- [42] M.E. Orazem, B. Tribollet, *The Electrochemical Society Series*, John Wiley & Sons, Inc, 2017.
- [43] C. Cao, On the impedance plane displays for irreversible electrode reactions based on the stability conditions of the steady-state-I. One state variable besides electrode potential, *Electrochim. Acta* 35 (1990) 831–836.
- [44] N. Perez, *Electrochemistry and Corrosion Science*, second ed., Springer, Switzerland, 2004.
- [45] J. Basumatary, R.J.K. Wood, Synergistic effects of cavitation erosion and corrosion for nickel aluminium bronze with oxide film in 3.5% NaCl solution, *Wear* 376-377 (2017) 1286–1297.
- [46] S. Hattori, T. Itoh, Cavitation erosion resistance of plastics, *Wear* 271 (2011) 1103–1108.
- [47] Y. Liu, D.L. Duan, S.L. Jiang, S. Li, Preparation and its cavitation performance of nickel foam/epoxy/SiC co-continuous composites, *Wear* 332-333 (2015) 979–987.
- [48] G. Bolelli, A. Milanti, L. Lusvarghi, L. Trombi, H. Koivuluoto, P. Vuoristo, Wear and impact behaviour of high velocity air-fuel sprayed Fe-Cr-Ni-B-C alloy coatings, *Tribol. Int.* 95 (2016) 372–390.
- [49] V. Matikainen, H. Koivuluoto, P. Vuoristo, J. Schubert, Š. Houdková, Effect of nozzle geometry on the microstructure and properties of HVAF-sprayed WC-10Co4Cr and Cr3C2-25NiCr coatings, *J. Therm. Spray Techn.* 27 (2018) 680–694.
- [50] H. Koivuluoto, G. Bolelli, A. Milanti, L. Lusvarghi, P. Vuoristo, Microstructural analysis of high-pressure cold-sprayed Ni, NiCu and NiCu + Al<sub>2</sub>O<sub>3</sub> coatings, *Surf. Coat. Tech.* 268 (2015) 224–229.
- [51] G.O.H. Whillock, B.F. Harvey, Ultrasonically enhanced corrosion of 304L stainless steel II: the effect of frequency, acoustic power and horn to specimen distance, *Ultrason. Sonochem.* 4 (1997) 33–38.
- [52] G. Bolelli, R. Giovanardi, L. Lusvarghi, T. Manfredini, Corrosion resistance of HVOF-sprayed coatings for hard chrome replacement, *Corros. Sci.* 48 (2006) 3375–3397.
- [53] G.C. Saha, T.I. Khan, G.A. Zhang, Erosion-corrosion resistance of microcrystalline and near-nanocrystalline WC-17Co high velocity oxy-fuel thermal spray coatings, *Corros. Sci.* 53 (2011) 2106–2114.
- [54] A. Lekatou, D. Sioulas, A.E. Karantzalis, D. Grimanellis, A comparative study on the microstructure and surface property evaluation of coatings produced from nanostructured and conventional WC-Co powders HVOF-sprayed on Al7075, *Surf. Coat. Tech.* 276 (2015) 539–556.
- [55] A.B. Oliveira, A.C. Bastos, C.M. Fernandes, C.M.S. Pinho, A.M.R. Senos, E. Soares, J. Sacramento, M.L. Zheludkevich, M.G.S. Ferreira, Corrosion behaviour of WC-10% AISI 304 cemented carbides, *Corros. Sci.* 100 (2015) 322–331.
- [56] Y. Wang, Y.G. Zheng, W. Ke, W.H. Sun, W.L. Hou, X.C. Chang, J.Q. Wang, Slurry erosion-corrosion behaviour of high-velocity oxy-fuel (HVOF) sprayed Fe-based amorphous metallic coatings for marine pump in sand-containing NaCl solutions, *Corros. Sci.* 53 (2011) 3177–3185.
- [57] S. Kim, S. Lee, S. Chong, Electrochemical characteristics under cavitation-erosion for STS 316L in seawater, *Mater. Res. Bull.* 58 (2014) 244–247.